Water-soluble pillar[5]arene sulfo-derivatives self-assemble into biocompatible nanosystems to stabilize therapeutic proteins

Dmitriy N. Shurpik, [†]* *Yulia I. Aleksandrova,* [†] *Olga A. Mostovaya,* [†] *Viktoriya A. Nazmutdinova,* [†] *Pavel V. Zelenikhin,* [‡] *Evgenia V. Subakaeva,* [‡] *Timur A. Mukhametzyanov,* [†] *Peter J. Cragg,* [††] *Ivan I. Stoikov* [†]*

[†]A.M.Butlerov Chemical Institute, Kazan Federal University, 420008, Kremlevskaya Street, 18, Kazan, Russian Federation

[‡] Institute of Fundamental Medicine and Biology, Kazan Federal University, 420008 Kremlevskaya, 18, Kazan, Russian Federation

[††] School of Applied Sciences, University of Brighton, Huxley Building, Moulsecoomb, Brighton, East Sussex BN2 4GJ, UK.

Abstract

Pillar[5]arenes containing sulfonate fragments have been shown to form supramolecular complexes with therapeutic proteins to facilitate targeted transport with an increased duration of action and enhanced bioavailability. Regioselective synthesis was used to obtain a water-soluble pillar[5]arene containing the fluorescent label FITC and nine sulfoethoxy fragments. The pillar[5]arene formed complexes with the therapeutic proteins binase, bleomycin, and

lysozyme in a 1:2 ratio as demonstrated by UV-vis and fluorescence spectroscopy. The formation of stable spherical nanosized macrocycle / binase complexes with an average particle size of 200 nm was established by dynamic light scattering and transmission electron microscopy. Flow cytometry demonstrated the ability of macrocycle / binase complexes to penetrate into tumor cells where they exhibited significant cytotoxicity towards A549 cells at 10^{-5} - 10^{-6} M while maintaining the enzymatic activity of binase.

Introduction

Over the past 50 years significant progress has been made in the fight against many forms of cancer, from establishing the mechanism of their occurrence to developing a methodology for their treatment. However cancers remain some of the most dangerous fatal diseases in the world.[1] The concept of protein therapy for oncological diseases has been developed and actively used over the past decades.[2] Following the rapid development of proteomics and protein engineering a large number of methods and drugs for protein-based cancer therapy have been created, including oligopeptides, bacteriocins, non-ribosomal peptides, toxins, cytokines, antibodies and vaccines.[3,4] A characteristic feature of anticancer protein drugs is their specific activity and low toxicity. However low stability bioavailability and membrane impermeability in combination with high immunogenicity severely limit the use of protein-based anticancer preparations.[3,5]

In recent years there has been a growing research interest in cytotoxic RNases of various organisms, such as the cationic proteins of eosinophils,[6] onconase and extracellular ribonucleases of bacilli,[7] due to the selective cytotoxicity of these enzymes in relation to cancer cells.[8] One such RNase, Bacillus pumilus RNase (binase), inhibits the proliferation of human leukemic Kasumi-1 cells, lung adenocarcinoma cells, ovarian and breast cancer cells.[9]

Previously it was shown that the binase stops the processes that are necessary for the survival of cancer cells, but does not reduce the viability of non-malignant cells. [10]

The main advantage of using cytotoxic RNases is the structural organization of enzymes, which determines their penetration and interaction with cancer cell components,[11] however, the protein nature of ribonucleases leads to a decrease in the stability and duration of the protein preparation. The solution to this problem can be the use of nanocarriers as components of the drug delivery system (DDS), which will provide an increase in stability, bioavailability and permeability, as well as a decrease in immunogenicity, which opens up prospects for the use of RNases in clinical practice.

Systems based on macrocyclic compounds occupy a special place among DDS. The presence of a macrocyclic cavity, along with their polyfunctionality and pre-organized structures, makes these compounds common components in DDS.[12] One class of macrocycles, the pillar[5]arenes, have been shown to fuctional as DDS components for anticancer drugs.[13-17] Pillar[5]arenes have a number of attractive characteristics, such as their ease of preparation and functionalization of the macrocyclic platform, [18] the controlled size of the macrocyclic cavity due to varying the length of substituents,[19] their low toxicity[20] and ability to dissolve in water.[21] The additional introduction of a fluorescent label into this platform allows them to be used as fluorescent sensors [22,23] for tumor imaging in photodynamic-photothermal therapy.[24]

In this work we have developed an original strategy to regioselectively functionalize the pillar[5]arene platform, yielding water-soluble derivatives containing a fluorescent label, as DDS components to deliver and prolong the action of the therapeutic antitumor ribonuclease binase.

Results and Discussion

We proposed that the formation of nanostructured supramolecular complexes based on binase and water-soluble pillar[5]arenes would increase the efficiency of binase, reduce its cytotoxicity for other organs and tissues, and increase the metabolic stability of the protein preparation, The resulting systems would improve the stability and biocompatibility of binase, as well as increase the efficiency and safety of immunomodulatory therapy with protein drugs based on RNases. To implement this idea it was necessary to select the conditions for the controlled supramolecular self-assembly of the water-soluble macrocyclic platform pillar[5]arene and the enzyme.

Binase is a cationic extracellular guanyl-specific RNase of Bacillus pumilus [11] and should form effective complementary interactions with anionic polyfunctional derivatives of pillar[5]arene. Flow cytometry is a convenient method to assess the macrocycle's interaction with cells and characterize the cytotoxic action of complexes, however, the technique requires a fluorescent label. The most effective way to introduce such a label without changing the cytotoxicity of the protein preparation is the regioselective functionalization of the macrocyclic platform.[25] There are many literature examples of regioselective pillar[5]arene synthesis,[26-29] however there is little on the preparation of fluorescent-labeled water-soluble derivatives of the pillar[5]arene in high yields by this route. In this regard we have developed an approach for regioselective introduction of a fluorescent fragment by selective nucleophilic substitution of the SH-group of a BOC-protected 2-aminoethanethiol followed by the introduction of one fluorescein moiety through reaction with fluorescein isothiocyanate (FITC) (Scheme 1).

The introduction of thiafragments into the macrocyclic platform has been well studied for cyclodextrins,[30] calixarenes [31,32] and pillar[5]arenes.[33,20,21] However an important aspect of the reaction is overcoming the energy barrier to introduce the first and subsequent substituents. [34-36] It should be noted that the first stage of functionalization, to give the

monosubstituted derivatives, has the greatest energy barrier.[35] Introducing a single substituent into the macrocycle structure is a key step as high yields of target products are required. Many such pillar[5]arene derivatives display unique characteristics of complexation and aggregate into both supramolecular polymers [13] and associates.[14]

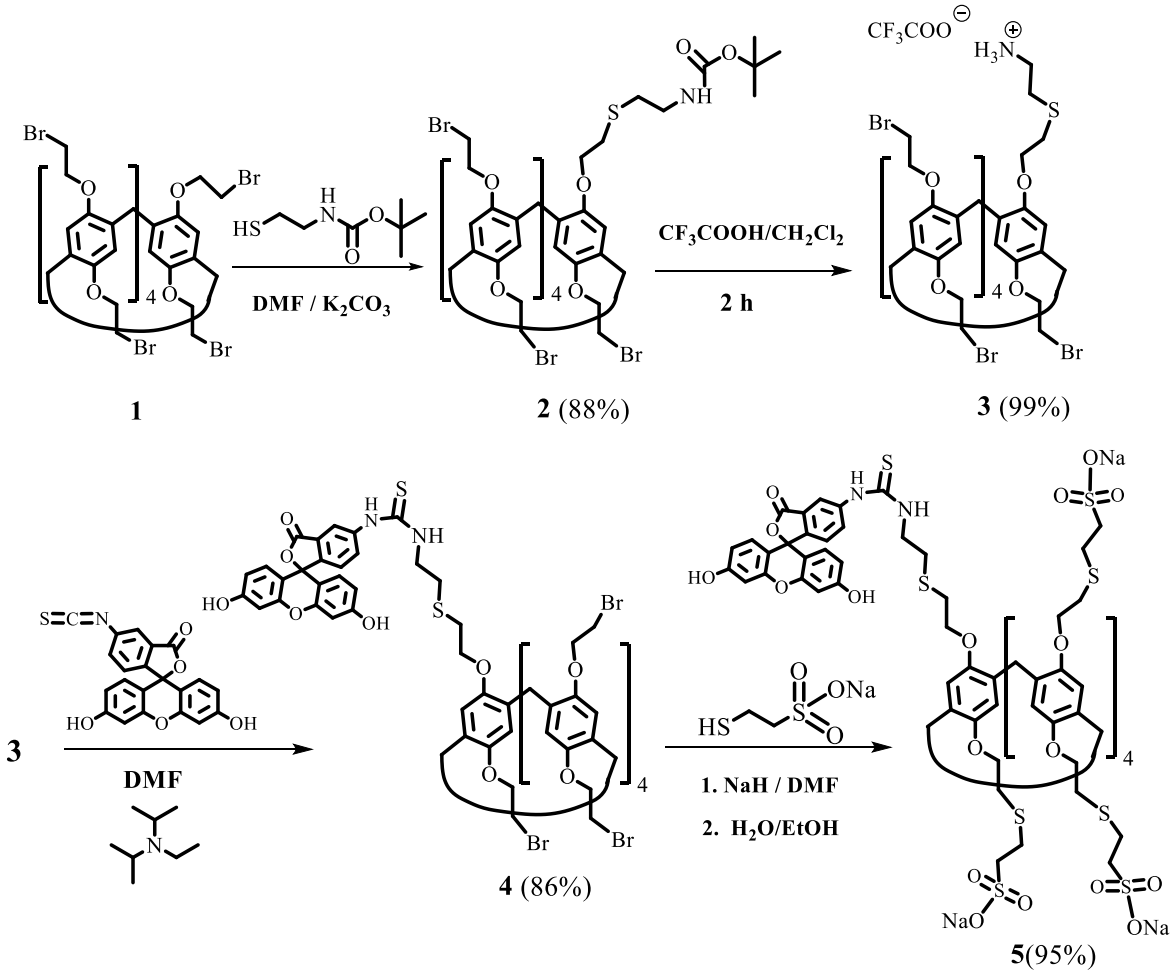

Scheme 1. Convergent strategy for synthesis of macrocycle **5** using fluorescein isothiocyanate (FITC).

Regioselective functionalization of the pillar[5]arene platform and synthesis of target macrocycles.

To obtain target macrocycle **5**, we started from decabromoethoxypillar[5]arene **1** prepared by the literature method.[37] Commercially available BOC-protected 2-aminoethanethiol was chosen as the thiafragment to be introduced. The reaction conditions were determined by

varying the temperature, reaction time, solvents and the ratio of reagents (ESI, Table S1) to ensure the regioselectivity of the thiol's reaction with pillar[5]arene **1** (Scheme 1).

The nucleophilic substitution in **1** proceeded in the highest yield with one equivalent of *tert*-butyl(2-mercaptoethyl)carbamate in dry DMF over 7 days at room temperature in the presence of potassium carbonate. Macrocycle **2** was isolated by column chromatography in 88%. *In situ* conversion to pillar[5]arene **3** was achieved by removing the protecting BOC group (Scheme 1) in the presence of trifluoroacetic acid in dichloromethane at room temperature. As the amino group in **3** was in the quaternarized salt form no covalent crosslinking occured between the bromoethoxy fragments and the amino group.

To introduce fluorescein, a widely used fluorescent label for biological imaging,[38] pillar[5]arene **3** was reacted with FITC (Scheme 1) in the presence of catalytic amounts of DIPEA in dry DMF at room temperature for 10 hours. This gave macrocycle **4** in 86%. Water-soluble macrocycle **5** was obtained by the direct thiolation method previously developed in our research group.[20] For this macrocycle **4** was introduced into a reaction with the bifunctional reagent sodium 2-mercaptoethanesulfonate in the presence of sodium hydride in dry DMF (Scheme 1). Thiolation proceeded at 90°C for 32 hours whereupon **5** was isolated in 95% yield. Macrocycles **1-5** were characterized by IR, ^{1}H, ^{13}C NMR spectroscopy, MALDI and ESI mass spectrometry and elemental analysis (ESI, Figure S1-S16).

Association of sulfo derivatives of pillar[5]arene with therapeutic proteins.

The abilities of macrocycle **5**, a decasulfo-substituted pillar[5]arene **6**,[20] and an acyclic analog, 1,4-disulfo-substituted benzene **7**,[21] to interact with therapeutic proteins was determined in buffer solutions (pH = 4.01; pH = 7.4 (physiological buffer); pH = 9.18) by UV-*vis* spectroscopy and dynamic light scattering (DLS) (Figure 1).

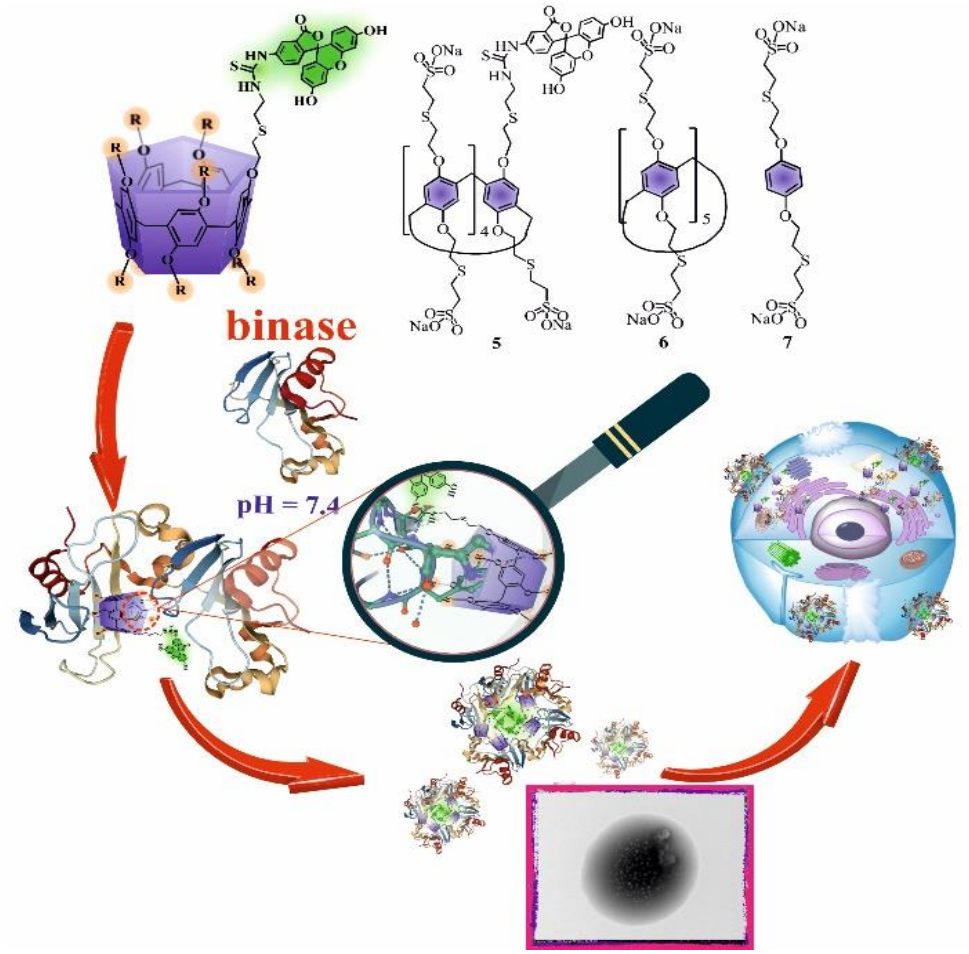

Figure 1. Structures of macrocycles **5-7** and a graphical representation the process of association of **5** with binase and its penetration into a cancer cell.[39,40]

An approach to the creation of nanostructured DDS systems based on non-toxic pillar[5]arenes [41] is currently being developed, however the use of pillar[5]arenes is limited by the size of the macrocyclic cavity and the number of functional groups. We have previously shown [21] that the introduction of thioether and sulfonate fragments makes it possible to increase the macrocyclic pseudo-cavity of the pillar[5]arene by increasing the length of the substituents. This makes it possible to interact with bulky guest molecules. In this regard, we hypothesized that polyfunctional pillar[5]arenes containing sulfonate fragments can be used as universal components of DDS, allowing effective interaction with cationic forms of protein therapy drugs through the formation of supramolecular associates.

Bleomycin, a commercially available drug for carcinoma and lymphoma chemotherapy;[42] *Bacillus pumilus* RNase (binase), exhibiting specificity for a number of carcinomas,[10,11] and a protein lysozyme similar in size and charge with antimicrobial properties [43] were selected as protein therapy drugs. It has been noted in the literature that the intracellular pH of a cancer cell and the pH of the microenvironment of tumor cells are both acidic [44,45] and vary between pH 5 and 6.9;[45] the highest pH level in the body is observed in pancreatic juice and juice colon which range from pH 7.8 to 9.0.[46] Thus, to study the processes of self-association of **5-7**, protein therapy drugs and their complexes, a pH range of 4.1 to 9.18 was chosen as optimal to study drug release under the acidic conditions in cancer cells and to allow the effect of pH on the destruction of the resulting aggregates to be determined.

The interaction of bleomycin with **5** was determined at pH 7.4 by UV-*vis* spectroscopy. The absorption spectra exhibit a weak hyperchromic effect at 295 nm (ESI, Figure S18). The association constant was established by spectrophotometric titration of a system in which the concentration of bleomycin was varied (3.33×10^{-6}-5×10^{-5} M) at a constant concentration of **5** (1×10^{-5} M). The association constant was calculated based on the analysis of binding isotherm data by BindFit.[47,48] The data obtained were consistent with a 1:2 binding model (5 / bleomycin) (ESI, Figure S17b). The association constants of **5** with bleomycin were $K_{ass1:1}$= 140 M^{-1} and $K_{ass1:2}$= 773599 M^{-1} (Table 1). Analysis based on 1:1 and 2:1 stoichiometries gave binding constants with a large error, confirming the 1:2 model (ESI, Figure S17).

The lysozyme interaction with both **5** and **6** was observed in phosphate buffer at the physiological pH of 7.4. The absorption spectra for the both macrocycles showed a hyperchromic effect at 292 nm (ESI, Figure S21, Figure S25). The hyperchromic effect was also observed at 502 nm for compound **5**. When the concentration of lysozyme was increased to 5×10^{-4} - 5×10^{-5} M with either **5** or **6**, a significant baseline rise was observed in the UV-*vis* spectra, indicating an increase in light scattering due the processes of aggregation (ESI,

Figure S21, Figure S25). Analysis of the binding isotherms obtained using BindFit showed that complexation only occurred for 5. The stoichiometry for **5** / lysozyme was found to be 1:2 with $K_{ass1:1}$= 47 M^{-1} and $K_{ass1:2}$ = 5728245 M^{-1} (Table 1, ESI, Figure S20b). Processing of the spectrophotometric titration data for **6** / lysozyme by BindFit was unsuccessful due to the strong aggregation of the system. Linearization of the curve in coordinates lg($C_{complex}/C_{host}$) - lg ($C_{lysozyme}$) allowed the logarithm of the association constant of the complex to be calculated as 5.3 (Table 1, ESI, Figure S26). The 1: 2 stoichiometry for was **6** / lysozyme was determined by a Job's plot (ESI, Figure S27).

Table 1. Association constants of compounds 5-7 with proteins (bleomycin, lysozyme, binase) in phosphate buffer (pH = 7.4) based on a 1:2 compound / protein binding model.

Protein / Host	Bleomicin	Lysozyme	Binase
5	(1:1) 140 M^{-1} (1:2) 773599 M^{-1}	(1:1) 47 M^{-1} (1:2) 5728245 M^{-1}	(1:1) 455 M^{-1} (1:2) 529196 M^{-1}
6	-	(1:2) 199526 M^{-1}*	(1:1) 38 M^{-1} (1:2) 508964 M^{-1}
7	-	-	-

* Benesi-Hildebrand method, stoichiometry 1: 2

The interaction of macrocycles **5** and **6** with the ribonuclease binase was confirmed by spectrophotometric and fluorescence titration data in a buffer at pH 7.4 (Figure 2). In the interaction between binase and pillar[5]arenes **5** and **6** in phosphate buffer at pH 7.4 a hyperchromic effect was observed in UV-vis spectra at 493 nm (where binase does not absorb), 282 nm for pillar[5]arene **5** and 282 nm for pillar[5]arene **6** (ESI, Figure S29) (Figure 2c). Upon formation of complexes between **5** and binase, in addition to the hyperchromic effect, the absorption spectra show a bathochromic shift of the fluorescein absorption band at 493 nm by 7 nm (Figure 2c). Complexation was quantified by BindFit to give the stoichiometry of the **5** / binase and **6** / binase complexes as 1: 2 (macrocycle: binase) with association constants of $K_{ass1:1}$= 445 M^{-1} and $K_{ass1:2}$= 529196 M^{-1} (for **5** / binase);

$K_{ass1:1}$= 38 M^{-1} and $K_{ass1:2}$= 508964 M^{-1} (for **6** / binase) (Table 1, ESI, Figure S23b, Figure S28b).

Additionally it was shown that model compound **7** does not interact with the selected drugs (Table 1), which confirms the key role of the macrocyclic platform in binding. The values of the association constants of the macrocycles **5** and **6** with the protein preparations are similar (Table 1) but the fluorescent label of **5** makes it convenient for use in tumor imaging systems.

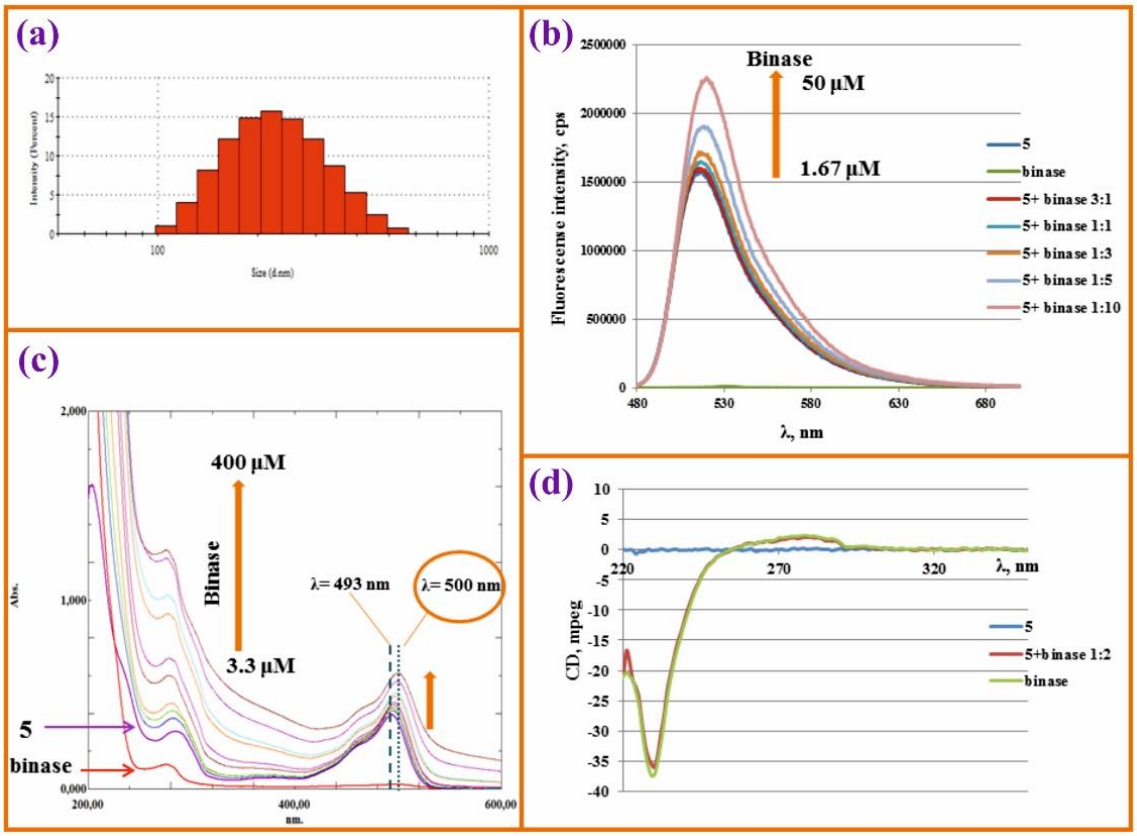

Figure 2. (a) Size distribution of the particles by intensity for **5** (10^{-5})/ binase (2×10^{-5} M) in buffer with pH = 7.4 (d =2 00.6 ± 9.6 nm, PDI= 0.12 ± 0.01); (b) Fluorescence spectra of **5** (5 μM) with 0 μM–50 μM concentrations of binase in buffer at pH 7.4; (c) UV-vis spectra of mixtures of **5** (1×10^{-5}M) with different concentrations of binase in buffer at pH 7.4; (d) Circular dichroism spectra of pillar[5]arene **5** (1×10^{-5}), binase (2×10^{-5}), and the complex of **5** (1×10^{-5}) with binase (2×10^{-5}) in buffer at pH 7.4.

It is known that pillar[5]arene derivatives are capable of selective interactions, self-assembly, and aggregation with amino acids [49,50] with the formation of various supramolecular assemblies in water.[51] In this regard the complexes formed by macrocycles **5** and **6** with proteins, in this case bleomycin, lysozyme and binase, can have a number of attractive properties, such as prolongation of the action of an antitumor agent, as well as visualization and pH-sensitive release.

Aggregation of macrocycles **5, 6** and model compound 7 with bleomycin, lysozyme, binase in a 1: 2 (macrocycle / agent) stoichiometry was studied by DLS in buffer solutions at pH 4.01, 7.40 and 9.18) and over the concentration range of 10^{-4}-10^{-6} M. Macrocycles **5** and **6**, and model compound **7**, did not form self-associates under any of these conditions (ESI, Table S2, Figure S31-33). The formation of unstable associates of nanometer sizes with a high polydispersity index (pH = 4.01-9.18) (ESI, Table S2, Figure S34, Figure S35) was observed in the case of solutions of bleomycin, lysozyme and binase.

The binding of lysozyme to macrocycles **5** and **6** was accompanied by the formation of submicron aggregates (ESI, Table S2, Figure S36, Figure S37). Precipitation occured across the entire pH range with an increase in the concentration from 10^{-6} M to 10^{-4} M of **5** and **6** in the macrocycle / lysozyme mixture. The smallest aggregates, at 264 nm, were formed at pH 7.4 with a ζ-potential of -8.7 mV for **6** / lysozyme. Aggregates with an average hydrodynamic diameter of 774 nm formed from **5** / lysozyme with a polydispersity index of 0.25 and a ζ-potential of -7.2 mV (Table 2).

Table 2. Aggregates of 5 to 7 with bleomicin, lysozyme or binase determined by DLS

Ratio H: G	**C_H, M**	**C_G, M**	**$Z_{average}$ (d), nm**	**PDI**	**ζ-potential, mV**	**buffer, pH**
7: lysozyme	10^{-5}	2×10^{-5}	**174±31**	0.51±0.11	-	**7.4**
	10^{-5}	2×10^{-5}	**167±40**	0.58±0.17	-	**4.01**
1:2	10^{-5}	2×10^{-5}	368 ±24	0.36±0.05	-2.7±0.9	**9.18**

6: lysozyme	10^{-6}	2×10^{-6}	**264±33**	0.36±0.05	**-8.7±0.6**	**7.4**
	10^{-6}	2×10^{-6}	1013±134	**0.26±0.02**	4.3±0.8	**4.01**
1:2	10^{-6}	2×10^{-6}	486±78	**0.23±0.02**	**-5.5±0.7**	**9.18**
5: lysozyme	10^{-6}	2×10^{-6}	774±80	**0.25±0.02**	**-7.2±0.5**	**7.4**
	10^{-6}	2×10^{-6}	995±80	0.42±0.07	4.4±1.2	**4.01**
1:2	10^{-6}	2×10^{-6}	1115±103	0.30±0.02	**-7.76±0.01**	**9.18**
7: binase	10^{-5}	2×10^{-5}	501±74	0.55±0.09	-	**7.4**
	10^{-5}	2×10^{-5}	345±113	0.55±0.15	-	**4.01**
1:2	10^{-6}	2×10^{-6}	**141±19**	0.43±0.06	**-10.3±0.6**	**9.18**
6: binase	10^{-5}	2×10^{-5}	**188±15**	**0.19±0.03**	-4.9±0.8	**7.4**
	10^{-5}	2×10^{-5}	568±126	0.59±0.09	-	**4.01**
1:2	10^{-5}	2×10^{-5}	**153.4±4.6**	**0.14±0.02**	**-13.9±1.1**	**9.18**
5: binase	10^{-5}	2×10^{-5}	**200.6±9.6**	**0.115±0.007**	**-10.3±0.6**	**7.4**
	10^{-6}	2×10^{-6}	**167.4±6.2**	**0.22±0.03**	**-6.1±0.3**	
1:2	10^{-5}	2×10^{-6}	1416±102	0.45±0.06	-	**4.01**
	10^{-5}	2×10^{-5}	**214±67**	0.53±0.07	-	**9.18**

In the case of binase the formation of complexes with macrocycles **5** and **6**, having low PDI values and particle sizes up to 200 nm, was observed (Table 2, ESI, Table S2, Figure S38, Figure S39). The most stable complexes of the macrocycle **5**, **6** / binase systems were observed at pH = 7.4 and a macrocycle concentration of 10^{-5} M. The average hydrodynamic diameter was 200 nm (PDI = 0.115 ± 0.007) (Figure 2a) and a ζ-potential of -10.3 mV was found for the macrocycle **5** / binase complexes. The particle size corresponded to 188 nm (PDI = 0.192 ± 0.026) and a ζ-potential of -4.9 mV was found for the **6** / binase system (Table 2, ESI, Table S2, Figure S38). The formation of binase complexes with **5** or **6** was observed at neutral and alkaline pH; however the formation of polydisperse macrocycle / binase systems was observed in an acidic buffer at pH 4.01 (Table 2, ESI, Table S2, Figure

S40). Thus it can be assumed that the release of the therapeutic proteins and the destruction of the nanoscale associates can be triggered upon the transition of the **5, 6** / binase system to acidic pH.

In the case of the **5** / binase system, solutions with a component ratio of 10: 1, 5: 1, 2: 1, 1: 1, 1: 2, 1: 5, 1:10, 1: 100 were also studied at a macrocycle concentration of 10^{-5} M at physiological pH. The formation of aggregates is observed only with excess binase and the polydispersity of the system increases with an excess of macrocycle **5** in the complex solution (Table 3, ESI, Figure S41, Figure S42).

Table 3. Aggregation of 5 with binase in buffer at pH 7.4

Ratio H:G	**C $_5$, M**	**C $_{binase}$, M**	**Z $_{average}$ (d), nm**	**PDI**
1:10	10^{-7}	10^{-6}	127±8	0.20±0.02
1:10	10^{-6}	10^{-5}	100.7±3.2	0.36±0.03
1:10	10^{-5}	10^{-4}	129.6±1.4	0.26±0.01
1:5	10^{-5}	$5x10^{-5}$	250.0±1.5	0.21±0.01
1:2	10^{-5}	$2x10^{-5}$	**245.5±2.9**	**0.15±0.02**
1:1	10^{-5}	10^{-5}	771±17	0.26±0.02
2:1	10^{-5}	$5x10^{-6}$	171.2±2.5	0.40±0.03
5:1	10^{-5}	$2x10^{-6}$	80.1±4.3	0.43±0.01
10:1	10^{-5}	10^{-6}	119±9	0.56±0.10
100:1	10^{-5}	10^{-7}	269±219	0.5±0.29

It should be noted that the model compound **7** did not form stable complexes with any of the proteins studied (Table 2). The interaction of bleomycin with **5** and **6** was evident through the formation of stable complexes in buffer, however, these did not form across the entire concentration and pH ranges studied (ESI, Table S2) which may be due to structural differences between the proteins. For example, the binding site of the substrate for guanine-

specific RNase-binase includes amino acids Lys26, Glu72, Arg82, Arg86, and His101 [52] with Glu72 and His101 responsible for direct binding to the substrate.[53,54] These amino acids are also present in the structure of lysozyme, however, here the active sites include Glu228, Asp244 in the first domain and the Asp244-Tyr dipeptide in the second.[55] Bleomycin contains Thr and His residues but Glu is absent. Hence it can be assumed that, in addition to ion-ionic interactions, pillar[5]arenes form inclusion complexes by binding to amino acids that are part of active protein binding sites for binase, bleomycin, and lysozyme. The absence of complexes of the macrocycles **5** and **6** with bleomycin can be explained by the relatively small size of the bleomycin molecule and a much smaller number of active binding sites than are present in lysozyme or binase.

We obtained the ^{1}H, 2D ^{1}H-^{1}H NOESY NMR spectra of **5**, histidine (His) and **5** / His in a 1:1 ratio (10^{-3} M) (Figure 3) to confirm this hypothesis. Histidine was chosen as one of the main amino acids that make up the active binding sites of binase and bleomycin, and is also present in the lysozyme molecule. Thus in the ^{1}H NMR spectrum of the **5** / His mixture in a 1:1 ratio (10^{-3} M), a shift of the signals of the aromatic protons of the imidazole fragment to the region of strong fields ($\Delta\delta \sim 0.2$ ppm) is observed, which indicates the incorporation of the His imidazole residue into the macrocyclic cavity of the pillar[5]arene **5** (ESI, Figure S43). Additionally this fact was confirmed by 2D ^{1}H-^{1}H NOESY NMR spectroscopy data (Figure 3). Corresponding cross-peaks were found between the aromatic protons of the imidazole fragment and the protons of the aryl fragments of the macrocycle 5 (Figure 3).

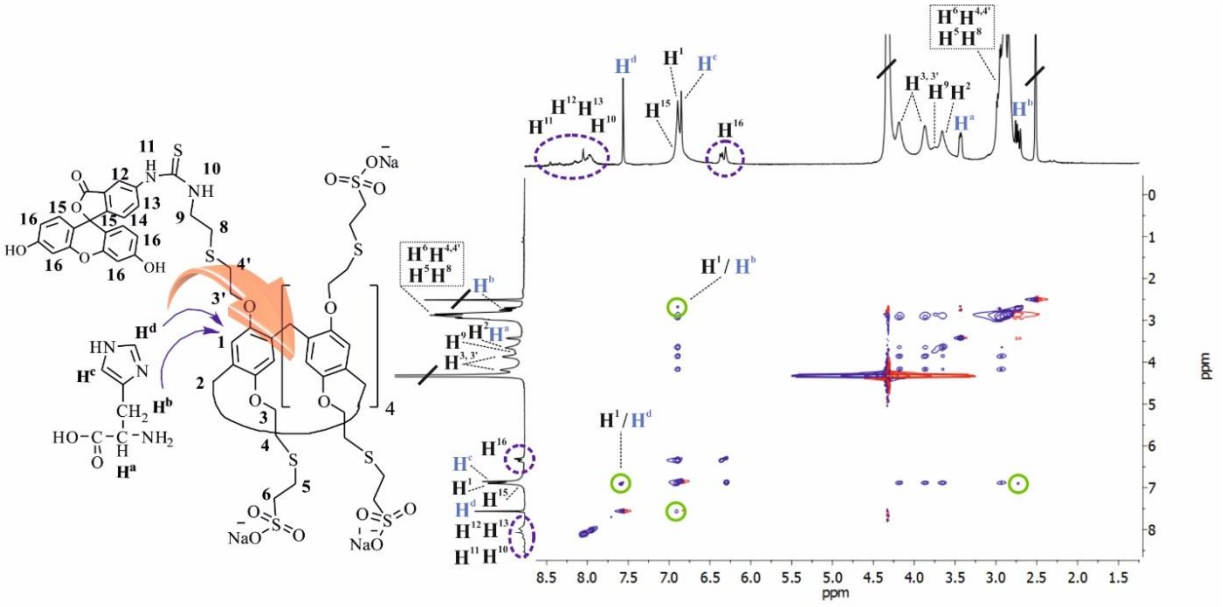

Figure 3. The 2D ^{1}H-^{1}H NOESY NMR spectrum of the **5** / histidine complex (1:1, 1×10^{-3} M) in D_2O/DMSO-d_6 = 1:1 at 25 °C.

To further probe the nature of the complex with pillar[5]arene **5** with binase, docking was simulated using molecular mechanics. The structure of binase - sulfate complex is an α,β-dimer with two anions per protein molecule.[56] Sulfur - sulfur distances within each molecule were 9.15 Å and 9.13 Å; those between molecules were 10.07 and 19.67 Å. When fully extended, the furthest distances between sulfur atoms in **5** is calculated to be 20.40 Å which suggested a good fit for a bridging pillar[5]arene that also gives the 2:1 stoichiometry determined spectroscopically. Four terminal sulfate groups were configured to fit in the sulfate binding domains and the geometry of the complex optimized. This resulted in the pillar[5]arene bridging the two protein molecules while forming a pseudorotaxane with His-108. With the pillar[5]arene bound in a cleft between the two protein moieties, the fluorescein group is available to act as a fluorescent label. Figure 4 illustrates how **5** can occupy this cleft while being anchored to sulfate binding sites in the binase α,β-dimer.

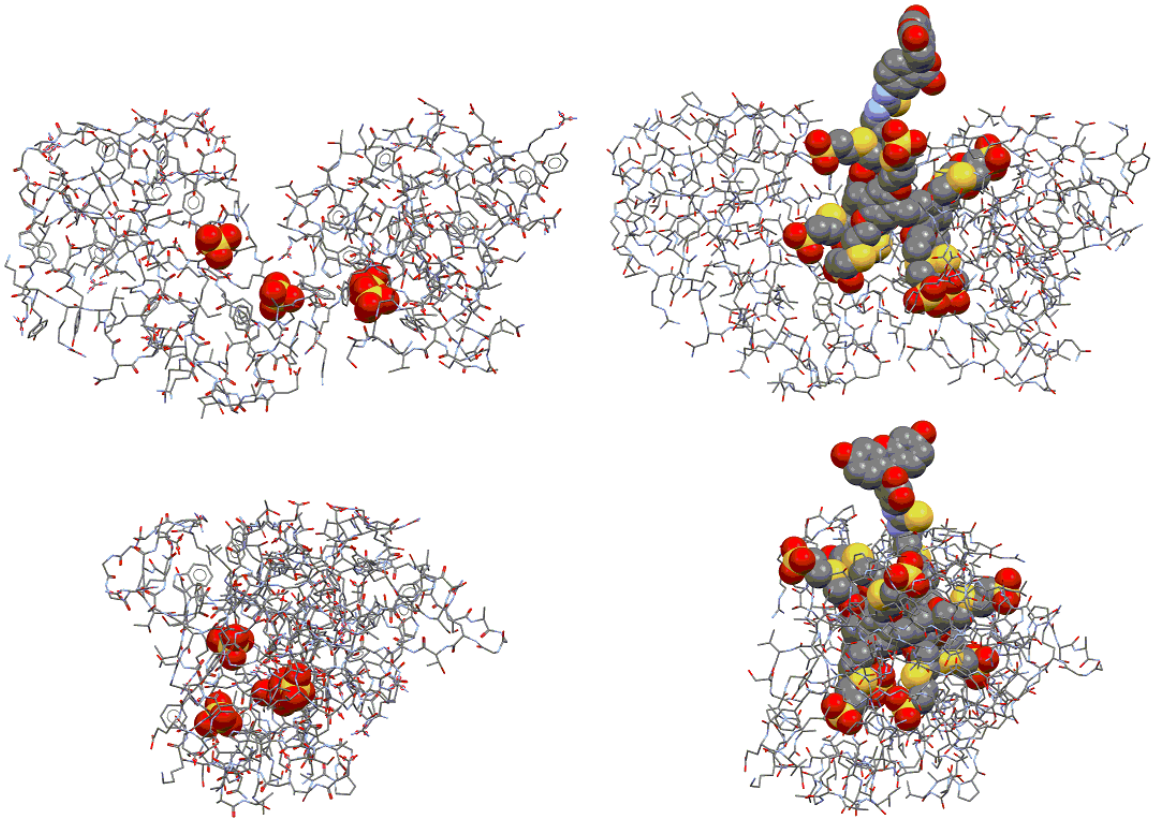

Figure 4. Structures of the binase α,β-dimer (left) with bound sulfates and its geometry optimized complex with **5** (right) (hydrogen atoms removed for clarity).

The literature describes the preparation of fluorescently-labeled proteins by binding the protein to a fluorescent substrate [57] thus the presence of a fluorescein tag in the structure of **5** makes it possible to study the structure of the resulting complex by fluorescence spectroscopy. Since strong aggregation of macrocycle **5** with lysozyme was observed, there were no spectral changes at the wavelength corresponding to the absorption maximum of fluorescein in the UV-vis spectra of **5** with bleomycin. The only feature observed at pH 7.4 due for the 5 / binase system was associated with the emission wavelength of fluorescein.

Analyzing the data obtained by UV-vis and fluorescence spectroscopy, it should first of all be noted that in the absorption spectrum for the fluorescein label, an absorption maximum is observed at 493 nm with a shoulder in the 460 nm region. This fact indicates the presence of its mono- and dianionic forms.[58] When **5** interacts with binase, the ratio of the absorption

bands of the fluorescein labeldoes not undergo significant changes. However, with an increase in the binase concentration (C_{binase} = 1.67×10^{-6} - 5×10^{-5} M) (Figure 2b), a sequential increase of the fluorescence for the **5**/protein complex is observed, accompanied by a slight bathochromic shift (5 nm). The very small Stokes shift for the fluorescein label in **5** (~ 20 nm) (Figure 2b, c) leads it to self-extinguish as a result of fluorescence resonance energy transfer (FRET).[59] In addition, the interaction with the protein reduces the possibility of energy transfer due to a decrease in the mobility of the fluorophore fragment, and the intensity of its fluorescence increases.[60] Moreover, as shown by DLS, compound **5** forms complexes in the presence of binase, while it is known that the incorporation of fluorescein derivatives into the inner region of the micelle is accompanied by an increase in their emission intensity.[61] Isolation of **5** from the buffer medium inside a negatively charged micelle prevents protonation of the dianionic form of fluorescein, leading to an increase in fluorescence.[62] Thus, the results unambiguously indicate the interaction between **5** and binase, through a change in the environment of the fluorescein label, implying that the pillar[5]arene is located inside the protein envelope.

The formation of the **5** / binase complex could significantly change the secondary and tertiary structure of a protein molecule. As a result the availability of active binding sites of the antitumor protein may be limited, and its biological activity might be reduced. Circular dichroism (CD) was used to investigate this possibility as it is sensitive to structural and conformational changes in protein molecules.[63] Upon the addition of **5** or **6** (10^{-5} M) to a protein solution (2 ×10^{-5} M), no deviations from the CD spectra of binase at the same concentration were recorded over the range of 220-300 nm (Figure 1d). Individually, compounds **5** and **6** gave no signals in the CD spectrum (Figure 1d). This fact clearly indicates the retention of the protein's secondary and tertiary structure during the formation

of the supramolecular complexes between **5** or **6** and binase (ESI, Figure S49) and the retention of the biological characteristics of the protein.

Transmission electron microscopy (TEM) was also used to study the structure and morphology of these complexes. Individually, macrocycles **5** and **6** and binase form shapeless aggregates according to TEM data (Fig. 5 and ESI, ESI, Figure S47, Figure S48). For the **5** / binase (Figure 5e) and **6** / binase complexes (Figure 5d), TEM images show ordered spherical aggregates, with an average diameter of 250 nm for **6** / binase and 200 nm for **5** / binase.

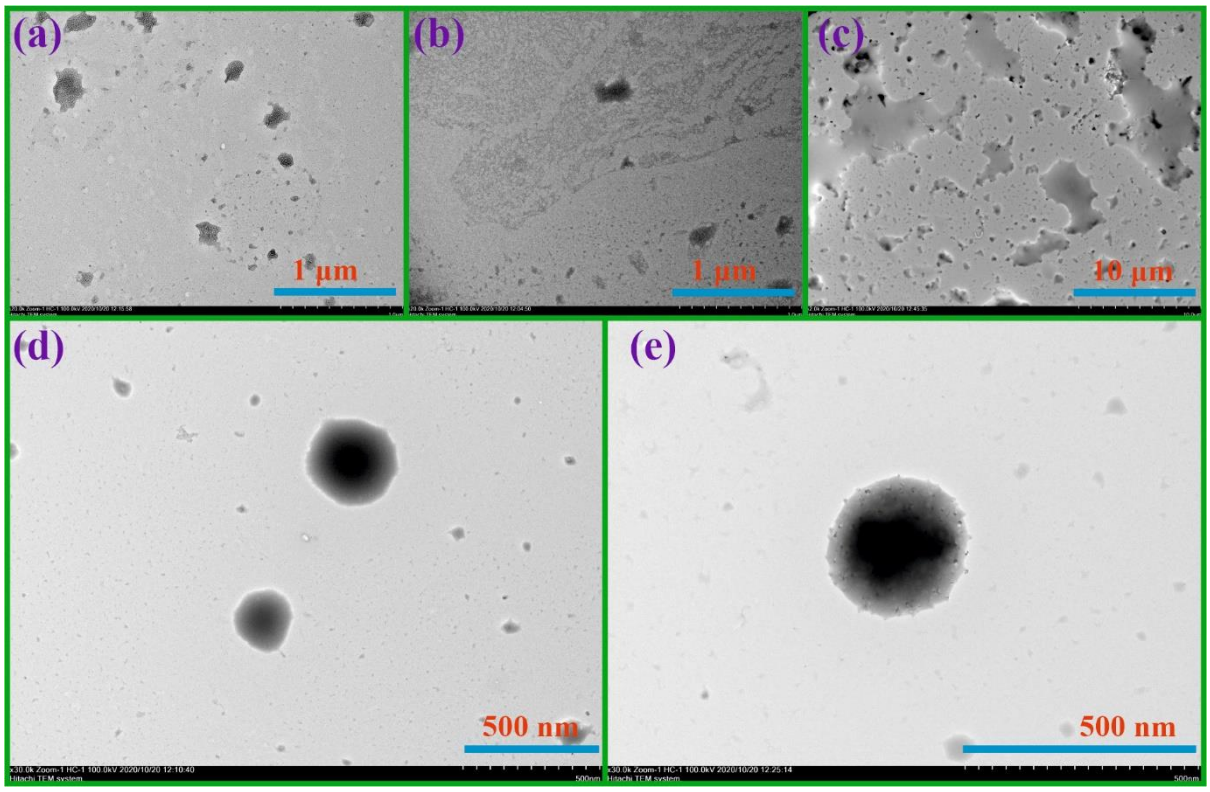

Figure 5. TEM images: (a) macrocycle **6** (10^{-5} M) in buffer at pH 7.4; (b) binase (2×10^{-5} M) in buffer at pH 7.4; (c) macrocycle **5** (10^{-5} M) in buffer at pH 7.4; (d) **6** (10^{-5} M) / binase (2×10^{-5} M) in buffer at pH 7.4 and (e) **5** (2×10^{-5} M) / binase (10^{-5} M) in buffer at pH 7.4

Based on the results obtained, the formation of spherical macrocycle / protein complexes occurs due to electrostatic interactions and structural complementarity of the bound pillar[5]arene with the configuration of the RNase. Based on TEM data, the spherical

particulate aggregates have centers comprised of densely packed macrocycles **5** or **6** with a protein outer layer. In this case the structure of the protein does not undergo conformational changes.

Biological activity of sulfo substituted macrocycles and their protein complexes.

The **5** and **6** / binase systems may not be applicable as DDS components for use *in vivo* due to the toxicity of the macrocycles. A series of experiments was carried out to assess changes in the viability of model adenocarcinoma human lung A549 cells when treated with pillar[5]arenes **5** and **6** to assess their toxicity. The ability of the pillar[5]arenes to inhibit the viability and proliferative activity of cells was determined using the MTT test [18] after incubation for 24 hours. Cell viability was expressed in relative units in comparison with a macrocycle-free control and it was found that pillar[5]arenes **5** and **6** did not reduce the viability of A549 cells over the entire range of investigated concentrations (0.5-50 μg / ml) (ESI, Figure S50, Figure S51).

The viability of A549 cells under the influence of the **5** or **6** / binase complexes was also assessed. No toxicity at 10^{-6} M was observed but a significant decrease in viability was recorded at 10^{-5} M (Figure 6a). The differences shown may be explained by the different sizes of complexes at concentrations of 10^{-5} M and 10^{-6} M. As can be seen from Figure 4, macrocycle **6** in combination with binase exhibited toxicity comparable to that of RNase solutions at the same concentration. The viability of A549 cells upon treatment with this system was 0.79 ± 0.08 a.u. and 0.73 ± 0.04 a.u. at 10^{-6} M and 10^{-5} M and that of the **5** / binase system was 0.89 ± 0.09 a.u., 0.83 ± 0.07 a.u. at 10^{-6} M and 10^{-5} M respectively.

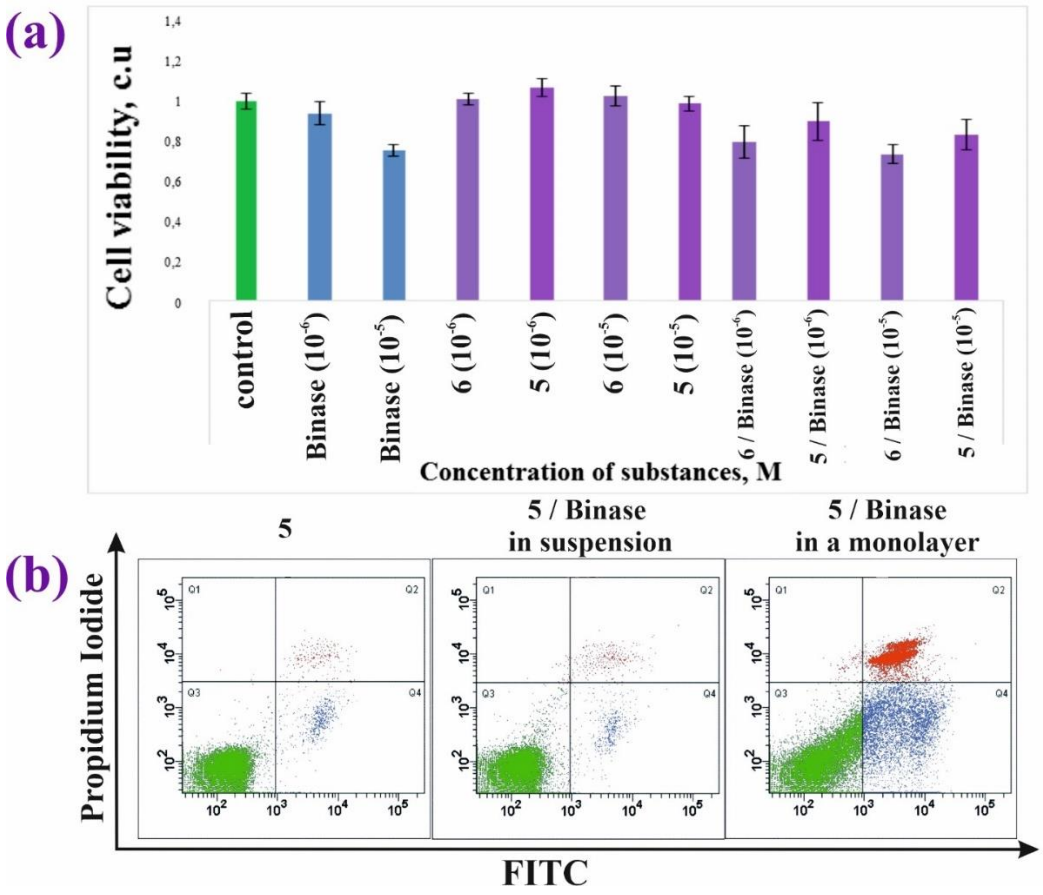

Figure 6. (a) Effect of macrocycles **5** and **6**, binase, and the **5** / binase and **6** / binase systems on the viability of A549 cells at 10^{-5} M and 10^{-6} M; (b) Cytofluorometric distribution of A549 cells after treatment with **5** (10^{-5} M) and **5** / binase (10^{-5} M) following 2 h in suspension and monolayer reflecting staining with fluorescein depending on the concentration of propidium iodide.

It was necessary to determine the complexes' abilities to penetrate into cells in order to determine the mechanisms of the cytotoxic action of **5** / binase complexes. The ability of pillar[5]arene **5** and the **5** / binase complex to penetrate into A549 cells was determined by flow cytometry (Figure 6b, ESI, Figure S52). We chose cytometry due to its high productivity, accuracy and sensitivity, exceeding those of fluorescence microscopy. The use of classical methods of staining cell lines with fluorescent dyes to visualize the penetration of the macrocycle / binase associates can lead to their premature destruction, since the literature has shown that pillar[5]arenes tend to form complexes with fluorescent dyes.[64, 65] The main

focus in the work is paid to the supramolecular system, which can reduce toxicity and increase the time of action of antitumor proteins (in particular binase). So the 5 / binase complex is ideal for these conditions. However the therapeutic effect itself is exerted by a protein molecule - binase. The antitumor effect and visualization of the intracellular distribution of binase have been studied in detail in earlier works.[10] Figure 6 shows the proportion of unstained viable cells by pillar[5]arene **5** (left lower quadrant), of stained viable cells by **5** (right lower quadrant), unstained dead cells (left upper quadrant) and stained by **5** (right upper quadrant) (Figure 6b). The cells were treated with agents as monolayers and in suspension. Upon incubation of cells in the presence of these substances in suspension, both the macrocycle and its complex with binase preferentially penetrated into dead cells. The proportion of viable cells stained with **5** did not change significantly, but the penetrating ability of **5**, alone, was higher than its complex with binase (Figure 6b). When a monolayer of cells was incubated in the presence of **5** and **5** / binase in the culture medium, living cells were penetrated (lower right quadrant). With this treatment the proportion of living cells stained with pillar[5]arene reached 50% of the total (Figure 6b).

Additionally we carried out a series of experiments to assess the viability of normal lung epithelial cells (LEC) in the presence of the 5 / binase complex. Normal LECs were insensitive to the complex, since there was no increase in the apoptotic population of LEC cells after 48 h of treatment with binase (100 and 300 μg / ml). The obtained results agree with the results presented in the literature.[10]

It should be noted that the cytotoxic properties of RNases largely depend on their enzymatic cleavage of phosphodiester bonds in RNA. The efficiency criterion for an active enzyme preparation placed in a DDS is the minimum loss of catalytic activity, and for antibodies, their immunological response.[66] Thus the determination of the enzymatic activity of the complexes **5** and **6** with binase showed a slight decrease in ribonucleolytic activity in

comparison with that of the protein alone. In this case, the activity of a solution of the complexes with an initial concentration of agents of 10^{-5} M was 80% of the maximum. This is in good agreement with the hypothesis of binding of the fragments of basic amino acids that are part of the active binding sites of binase to the macrocyclic cavity of the pillar[5]arene. However with an increase in the concentration of the macrocycle / binase complex to a concentration of 10^{-4} M, the systems showed only 33% (**6** / binase) and 43% (**5** / binase) of the catalytic activity of the RNase solution at the corresponding concentration. We assume that this is due to the ongoing processes of aggregation (ESI, Table S3). Due to the fact that the binase IC_{50} for a number of tumor cell lines is in the range 2.44×10^{-6} to 4.1×10^{-5} M,[8-11] a decrease in enzymatic activity at higher concentrations of the **5** and **6** complexes with binase may reduce the cytotoxic effects of the drug in relation to healthy cells. Thus the binase complexes, within the limits of their effective concentrations, can potentially prolong the action of the drug and lead to a longer lasting therapeutic effect.

Conclusions

The ability of the pillar[5]arenes containing sulfonate fragments to form supramolecular complexes with therapeutically active proteins was shown to increase their duration of action, bioavailability and targeted transport. Water-soluble pillar[5]arene **5** labeled with fluorescein and nine sulfoethoxy fragments was obtained for the first time by regioselective synthesis. Its application as a fluorescence sensor capable of imaging tumors for photodynamic-photothermal therapy was confirmed fluorescence spectroscopy. DLS has shown the formation of stable nanoscale complexes between macrocycle **5** or **6** and the antitumor protein binase. The formation of these nanosized associates was recorded at neutral and alkaline pH. However in an acidic buffer (pH 4.01), the formation of polydisperse macrocycle / binase systems was observed, making the release of the protein drug and destruction of the structure of the nanosized associates possible during the transition to acidic

pH. It was shown that the **5** / binase and **6** / binase complexes are spherical particles in aqueous solutions, with an average diameter of 250 nm for the complexes **6** / binase and 200 nm for **5** / binase by TEM. The ability of **5** / binase complexes to penetrate into tumor cells was assessed by flow cytometry. The **5** / binase and **6** / binase complexes exhibited significant cytotoxicity towards A549 cells in the concentration range of 10^{-5} to 10^{-6} M while maintaining the enzymatic activity of binase over this concentration range. These results open up opportunities for the development of new DDS systems containing protein anticancer drugs with prolonged action and sensitivity to external stimuli.

Materials and Methods

Materials

Most chemicals were purchased from Aldrich and used as received without additional purification. Organic solvents were purified in accordance with standard procedures.

Methods

Synthesis of the compounds 2-5.

Pillar[5]aren **1** were synthesized according to the literature procedure,[37] pillar[5]aren **6** were synthesized according to the literature procedure,[20] compound **7** were synthesized according to the literature procedure.[21]

4-[(tert-Butylcarbamoyl-2-sulfanedyl)ethoxy]-8,14,18,23,26,28,31,32,35-nona-[bromoethoxy]-pillar[5]arene (2).

Anhydrous K_2CO_3 (0.1 g, 0.72 mmol) with anhydrous DMF (10 ml) was placed in a round-bottom flask equipped with a magnetic stirrer. The solution was stirred while cooling in an ice bath. Then pillar[5]arene **1** 0.3 g (0.18 mmol) was added in one portion. Then, a solution of tert-butyl(2-thioethyl)carbamate 0.03 g (0.18 mmol) in 5 ml of DMF was slowly added to

the reaction mixture. The ice bath was removed and the temperature of the reaction mixture was brought to room temperature. The reaction was carried out for a week at room temperature in an argon atmosphere. After the reaction mixture was poured into distilled water. The resulting white oily precipitate was centrifuged, the aqueous solution was decanted, the precipitate was dissolved in 10 ml of methylene chloride and evaporated on a rotary evaporator. The residue was washed with hot hexane. The target macrocycle was isolated using silica gel column chromatography (CH_2Cl_2:ethyl acetate = 4:1). Product yield 0.2 g (88%), M.p.= 116 ºC. NMR ^{1}H ($CDCl_3$, δ, ppm., *J*/Hz): 1.45 s (9H, t-Bu), 2.72 t (2H, $^2J_{HH}$= 6.5 Hz, -SCH_2-), 2.93 (t, 2H, $^2J_{HH}$= 6.4 Hz, -CH_2S-), 3.33 (t, 2H, $^2J_{HH}$= 5.6 Hz, -$\underline{CH_2}$NH-), 3.63 (t, 18H, $^2J_{HH}$= 5.4 Hz, -CH_2Br), 3.84 (s, 10H, -CH_2-), 4.22 (t, 20H, $^2J_{HH}$= 6.8 Hz,-O$\underline{CH_2}CH_2S$-), 6.82-6.94 (m, 10H, ArH). NMR ^{13}C ($CDCl_3$, δ, м.д.): 28.56, 29.50, 30.86, 31.64, 32.96, 40.06, 68.34, 69.15, 116.26, 129.13, 149.79, 154.10. IR (ν, sm^{-1}) 2926(-C_{Ph}-H), 2860(-CH_2-), 1706(-C=O Amide I), 1659(-N-H Amide II), 1496(-CH_2-), 1309(C-NH-C Amide III), 1274(-CO-O-C$(CH_3)_3$), 1201(C_{Ph}-O-CH_2), 1099((-CO-O-C$(CH_3)_3$), 1071(C_{Ph}-O-CH_2). Mass-spectrum (MALDI-TOF): calculated [M^+] m/z = 1776.7, found [M+Na]$^+$ m/z = 1800.4.

4-[2-Ethoxythiaethanammonium]-8,14,18,23,26,28,31,32,35-nona-[bromoethoxy]-pillar[5]arene 2,2,2-trifluoroacetate (3).

In a round-bottom flask equipped with a magnetic stirrer, 0.22 g (0.13 mmol) of macrocycle **2** was dissolved in 3 ml of methylene chloride. Then added 0.3 ml of 2,2,2-trifluoroacetic acid. The reaction was carried out with stirring for 2 hours at room temperature in an argon atmosphere. After the reaction mixture was evaporated to dryness on a rotary evaporator. The product was used without further purification. Product yield 0.23 g (99%), M.p.= 122ºC. NMR ^{1}H (DMSO-*d*$_6$, δ, ppm, *J*/Hz): 2.81 (t, 2H, $^2J_{HH}$= 7.0 Hz, -$\underline{CH_2}$-NH_3^+), 2.99-3.06 (m, 4H, -CH_2SCH_2-), 3.67-3.80 (m, 10H, -CH_2-), 3.85 (t, 18H, $^2J_{HH}$= 4.8 Hz, -CH_2Br-), 4.04-4.44

(m, 20H, -O$\underline{CH_2}$-), 6.87-7.01 (m, 10H, ArH). NMR ^{13}C (DMSO-*d*$_6$, δ, ppm): 28.59, 29.99, 30.77, 32.52, 38.46, 67.64, 68.89, 115.30, 115.33, 128.75, 128.85, 128.87, 149.13, 149.24, 149.38. IR (v, sm^{-1}) 2927(-C$_{Ph}$-H), 2861(NH_3+,), 1672(-C=O Amide I), 1496(-CH_2-), 1457(C$_{Ph}$-C$_{Ph}$), 1278(C-F), 1198(C$_{Ph}$-O-CH_2), 1069(C$_{Ph}$-O-CH_2). Mass-spectrum (MALDI-TOF): calculated [M$^+$] m/z = 1788.7, found [M-CF_3COOH+H$^+$]$^+$ m/z = 1678.2.

4-[(Dioxofluoryl-4-thiocarbomoyl-2-sulfanedyl)ethoxy]-8,14,18,23,26,28,31,32,35- nona-[bromoethoxy]-pillar[5]arene (4).

In a round bottom flask equipped with a magnetic stirrer, 0.23 g (0.13 mmol) of macrocycle 3 and 0.1 g (0.26 mmol) of fluorescein isothiocyanate were dissolved in 7 ml of anhydrous DMF. Then 0.16 ml (0.92 mmol) of DIPEA was added. The reaction was carried out with stirring at room temperature for 10 hours in an argon atmosphere. After the reaction mixture was poured into distilled water (20 ml). The resulting orange oily precipitate was centrifuged, the aqueous solution was decanted, the precipitate was dissolved in 20 ml of methylene chloride and washed with distilled water (3×25 ml). Then the organic phase was separated and evaporated on a rotary evaporator. The target product was isolated by recrystallization from EtOH. Product yield 0.25 г (86%), M.p.= 205^{o}C. NMR ^{1}H (DMSO-*d*$_6$, δ, ppm, *J*/Hz): 2.70-2.90 (m, 2H, -CH_2-S-$\underline{CH_2}$-), 3.05 (t, 2H, $^2J_{HH}$= 6 Hz, $\underline{-CH_2}$-S-CH_2-), 3.76 (s, 10H, -CH_2-), 3.86 (t, 18H , $^2J_{HH}$= 4.5 Hz ,-$OCH_2\underline{CH_2}Br$), 4.0 (m, 2H, -$CH_2\underline{CH_2}NH$-), 4.06-4.51 (m, 20H ,-$\underline{OCH_2}CH_2$-), 6.52- 6.64 (m, 4H, Flu(H_{16})), 6.64- 6.70 (m, 2H, Flu(H_{15})), 6.87- 7.06 (m, 10H, ArH), 7.17 (d, 1H, $^2J_{HH}$= 8.1 Hz, Flu(H_{14})), 7.74 (d, 1H, $^2J_{HH}$= 7.7 Hz, Flu(H_{13})), 8.22 (m, 1H, -NH-, (H_{10})), 8.32 (s, 4H, Flu(H_{12})), 10.09 (m, 1H, -NH-, (H_{11})). NMR ^{13}C (DMSO-*d*$_6$, δ, ppm): 16.77, 18.13, 18.60, 28.55, 30.83, 35.85, 53.64, 68.73, 102.29, 109.72, 112.62, 115.17, 124.26, 126.32, 128.59, 129.11, 141.08, 149.03, 149.84, 151.93, 159.50, 162.40, 168.56. IR (v, sm^{-1}) 2926(-C$_{Ph}$-H), 1754(-C=O), 1606(-N-H Thioamide II), 1496(-CH_2-), 1456(C$_{Ph}$-C$_{Ph}$), 1385(-C=S), 1200(C$_{Ph}$-O-CH_2), 1107(-C=S), 1068(C$_{Ph}$-O-CH_2) Mass-spectrum (MALDI-

TOF): calculated [M+] m/z = 2063.7, found [M+Li+2H]+ m/z = 2073.1, [M-(Flu-NH)]+ m/z =1710.5.

4-[(Dioxofluoryl-4-thiocarbomoyl-2-sulfanedyl)ethoxy]-8,14,18,23,26,28,31,32,35-nona-[(thiaetansulfonate)ethoxy]- pillar[5]arene sodium salt (5).

To a round bottom flask equipped with a magnetic stirrer was added 0.23 g of NaH (60 % dispersion in mineral oil) in 3 ml of DMF. Then, while cooling in an ice bath, 0.36 g (2.18 mmol) of a solution of the sodium salt of 2-mercaptoethanesulfonic acid in 3 ml of DMF was added dropwise. Then a solution of macrocycle **4** 0.25 g (0.12 mmol) in 7 ml of anhydrous DMF was added dropwise to the reaction mixture at a temperature of 5-10 °C. The temperature was brought to room temperature and stirred for 30 minutes. Then the reaction mixture was heated for 32 hours at 90 °C. Then the reaction mixture was poured into 20 ml of cold ethyl alcohol. The precipitate that formed was filtered on a Schott funnel and washed with EtOH. The target product was isolated by recrystallization from EtOH and dried under reduced pressure over P_2O_5. Product yield 0.3 g (95%), M.p.= 225ºC (with decomposition). NMR ^{1}H (DMSO-*d*$_6$, δ, ppm, J/Hz): 2.67 (m, 2H, -$\underline{CH_2}CH_2NH$-), 2.70-2.92 (m, 38H, -CH_2S-, -$CH_2CH_2SO_3Na$), 3.68 (s, 10H, -CH_2-) 3.75-3.80 (m, 2H, -$CH_2\underline{CH_2}NH$-), 3.87-4.26 (m, 20H ,-O$\underline{CH_2}CH_2S$-), 5.78- 6.27 (m, 4H, Flu(H_{16})), 6.57- 6.76 (m, 2H, Flu(H_{15})), 6.83- 7.04 (m, 10H, ArH), 7.09- 7.23 (m, 1H, Flu (H_{14})), 7.83 (m, 1H, -NH-, (H_{10})), 7.94 (m, 1H, Flu(H_{13})), 8.08 (s, 4H, Flu(H_{12})), 8.32 (m, 1H, -NH-, (H_{11})). NMR ^{13}C (DMSO-*d*$_6$, δ, ppm): 27.38, 28.66, 31.38, 56.06, 67.55, 89.24, 102.40, 109.10, 114.61, 122.86, 128.28, 129.21, 130.46, 148.86, 151.72, 156.77, 157.79, 163.08, 180.82. IR (v, sm^{-1}) 3400(-OH), 2925(-C_{Ph}-H), 2865(-CH_2-), 1635(-C=O), 1573(-N-H Thioamide II), 1498(-CH_2-), 1462(C_{Ph}-C_{Ph}), 1406(-SO_3Na)), 1390(-C=S), 1330(C-NH-C Amide III), 1305(C_{Ph}-O-CH_2-), 1168(- SO_3Na), 1108(-C=S), 1045(C_{Ph}-O-CH_2-, -SO_3Na). Mass-spectrum (ESI): calculated [M] m/z = 2813.03, found [M-7Na^+]$^-$ m/z = 378.9, [M-9Na^+]$^-$ m/z = 289.6.

Characterization.

^{1}H NMR, ^{13}C NMR NMR spectra were obtained on a Bruker Avance-400 spectrometer ($^{13}C\{^{1}H\}$ - 100 MHz and ^{1}H - 400 MHz).Chemical shifts were determined against the signals of residual protons of deuterated solvent (DMSO-d_6,$CDCl_3$-d_6). The concentration of sample solutions was 3-5 %.

Attenuated total internal reflectance IR spectra were recorded with Spectrum 400 (Perkin Elmer) Fourier spectrometer. The IR spectra from 4000 to 400 cm^{-1} were considered in this analysis. The spectra were measured with 1 cm^{-1} resolution and 64 scans co-addition.

Elemental analysis was performed with Perkin Elmer 2400 Series II instrument.

Mass spectra (MALDI-TOF) were recorded on an Ultraflex III mass spectrometer in a 4-nitroaniline matrix. Melting points were determined using a Boetius Block apparatus. Electrospray ionization mass spectra (ESI) were obtained on an AmazonX mass spectrometer (Bruker Daltonik GmbH, Bremen, Germany). The measurements were carried out in the regime of positive ions registration in the range of *m/z* from 100 to 2800. The voltage on the capillary was - 4500 V. Nitrogen was used as the gas-drier with a temperature of 300 °C and a flow rate of 10 L·min[1]. The compounds were dissolved in acetonitrile to a concentration of 10^{-6} g/L. Data was processed using DataAnalysis 4.0 (Bruker Daltonik GmbH, Bremen, Germany).

Additional control of the purity of compounds and monitoring of the reaction were carried out by thin-layer chromatography using Silica G, 200 μm plates, UV 254.

Fluorescence.

Fluorescence spectra were recorded on a Fluorolog 3 luminescent spectrometer (Horiba Jobin Yvon). The excitation wavelength was selected as 485 nm. The emission scan range was 480-700 nm. Excitation and emission slits were 4 nm. Quartz cuvettes with optical path length of 10 mm were used. Fluorescence spectra were automatically corrected by the Fluoressence

program. The spectra were recorded in phosphate buffer (pH=7.4) with concentration of pillar[5]arenes 1 μM. The obtained molar ratio of pillar[5]arene **5** to binase was 1:10. The experiment was carried out at 293 K.

UV-vis spectroscopic studies.

UV-vis spectra were recorded using the Shimadzu UV-3600 spectrometer; the cell thickness was 1 cm, slit width 1 nm. Deionized water with a resistivity >18.0 MΩ cm was used to prepare the buffers (pH=4.01, pH=7.4, pH=9.18). Deionized water was obtained from a Millipore-Q purification system. The absorption spectra of the mixtures of compounds **5-7** (1×10^{-4}M) with bleomicin, lysozyme, binase were recorded after mixing the solutions at 298 K. The 1×10^{-4} M solution of the guest (bleomicin, lysozyme, binase (60, 75, 100, 150, 300, 600, 900, 1200, 1500, 1×10^{-4}) in phosphate buffer was added to 300 μL of the solution of **5-7** (1×10^{-4} M) in phosphate buffer and diluted to final volume of 3 mL with phosphate buffer. The UV spectra of the solutions were then recorded. The association constants of complexes were calculated as described below. Three independent experiments were carried out for each series. Student's t-test was applied in statistical data processing. The experiment was carried out according to the literature method. Stoichiometry of complexes was determined by Job's plot.

Dynamic Light Scattering (DLS).

The particle size and zeta potential was determined by the Zetasizer Nano ZS instrument at 20 °C. The instrument contains 4mW He-Ne laser operating at a wave length of 633 nm and incorporated noninvasive backscatter optics (NIBS). The measurements were performed at the detection angle of 173° and the software automatically determined the measurement position within the quartz cuvette. The 10^{-4} - 10^{-6} M aqueous solutions of the **5-7**, bleomicin, lysozyme, binase, **5** with different protein (bleomicin, lysozyme, binase) complex (concentration ratio 1:2) in different buffers (pH=4.01, pH=7.4, pH=9.18), **6** with different

protein (bleomicin, lysozyme, binase) complex (concentration ratio 1:2) in different buffers (pH=4.01, pH=7.4, pH=9.18), **7** with different protein (bleomicin, lysozyme, binase) complex (concentration ratio 1:2) in different buffers (pH=4.01, pH=7.4, pH=9.18). The concentration ratio of macrocycle **5** and binase in complexes was 10:1, 5:1, 2:1, 1:1, 1:2, 1:5, 1:10 and 1:100. Electrophoretic mobility of different samples was using a fold capillary cuvette (Folded Capillary Cell DTS1060, Malvern, U.K.). The experiments were carried out for each solution in triplicate.

Circular dichroism.

The circular dichroism was measured with the Jasco-1500 spectrophotometer in 1 mm thick quartz cuvettes (15 nm/min, 235–330 nm, slit width 1 nm, sampling step 1 nm, 3 scans co-addition). The 10^{-4} - 10^{-6} M aqueous solutions of the **5**, **6**, binase and complex with **5**, **6**/binase (concentration ratio 1:2) in buffer (pH=7.4). The experiments were carried out for each solution in triplicate.

Transmission Electron Microscopy (TEM).

TEM analysis of samples was carried out using the JEOL JEM 100CX II transmission electron microscope. For sample preparation, 10 μL of the suspension 10^{-5} M were placed on the Formvar/carbon coated 3 mm nickel grid, which was then dried at room temperature. After complete drying, the grid was placed into the transmission electron microscope using special holder for microanalysis.

Cytotoxicity studies.

The ability of macrocyclic compounds **5**, **6**, as well as complexes of pillar[5]arenes with binase, to inhibit the viability and proliferative activity of A549 cells was investigated using the MTT test according to.[67]

A549 cells were cultured in DMEM medium supplemented with 10% serum and 100 Units/ml of penicillin and streptomycin in a humid atmosphere with 5% CO_2 at 37°C. Cells

were seeded in 96-well plates at a concentration of 10^4 cells/well. After 24 hours of cultivation, the medium was removed from the wells and replaced with a fresh one with the addition of the test substances. The volume of the culture medium in the wells was 100 µl. After 24 h (in experiments with pillararens **5**, **6**) and 48 h (in experiments with pillararenes **5**, **6** with binase) incubation of cells in the presence of substances, the medium in the wells was replaced with a fresh one containing MTT at a concentration of 0.5 mg/ml. The cells were incubated with MTT for 4 hours at 37°C in an atmosphere of 5% CO_2. Then, the medium was aspirated from the wells and 100 µl of dimethyl sulfoxide was added thereto, after which it was incubated at 37°C for 15 min in the dark. The optical density of the formazan solution in the wells was measured using a plate reader (BioRad xMarkTM MicroplateSpectrophotometer, USA) at a wavelength of 570 nm. Three series of experiments were carried out with 5 replicates for each variant in the series.

Cytometry studies.

The ability of FITC-labeled compound **5** and its binase associate to penetrate into A549 cells was determined on a BD FACSCanto II flow cytometer. The assay was carried out after incubating cells in the form of a suspension and a monolayer for 2 hours at 37°C in the presence of the test compounds and subsequent staining with the fluorescent dye propidium iodide, which selectively stains dead cells.

In the suspension version, pillar[5]arene **5** and its associate with RNAse were introduced into 1 ml of a previously prepared suspension of A549 cells (2×10^5 cells/ml) in sterile cytometric tubes. The suspension was incubated with the agents for 2 h at 37°C in an atmosphere of 5% CO_2. Then the samples were stained with 5 µl of PI solution (5 mg/ml) for 2 minutes in the dark at room temperature and cytometric assessment of the presence of the fluorescent signal of the FITC-labeled macrocycle in dead and viable cells was performed.

In the variant with the treatment of pillar[5]arene **5** and its associate with the binase of the cell monolayer, the cells were pre-seeded in a 12-well plate at a concentration of 10^5 cells/well. After 24 h of cultivation, the medium was removed from the wells and replaced with a fresh one with the addition of the test substances. The volume of the culture medium in the wells was 1 ml. After 2h, the medium was taken from the plate and placed in individual centrifuge tubes to exclude the loss of dead cells separated from the monolayer. After the monolayer was washed with 1 ml PBS solution, trypsinized with the addition of 200 µl of 0.05% trypsin solution per well, the plate was incubated for 10 min at 37°C to destroy the monolayer. Then the cell suspension was transferred to the previously selected medium. Next, the cell suspension was centrifuged at 2000 rpm for 5 minutes at room temperature. After centrifugation, the liquid was decanted and resuspended in 1 ml of PBS solution. The cell suspension was transferred into cytometric tubes and the samples were stained with 5 µl of PI solution (5 mg / ml), kept in the dark at room temperature for 2 min, and cytometric analysis was performed. Cytometric data were processed using a specialized computer program FACSDiva.

Catalytic activity of binase.

The catalytic activity of binase in relation to the substrate - yeast RNA - was determined by the modified Anfinsen method.[68]

The samples under study were diluted 2000 times with distilled water with a dilution factor of no more than 20 (the first dilution was 10 times (20 µL of the sample + 180 µL of water); the second - 10 times, for a total of 100 (20 µL of the sample + 180 µL of water); the third - 20 times, for a total of 2000 times (10 µl of sample + 190 µl of water). To 25 µl of samples were added 100 µl of 0.5 M Tris-HCl buffer and 125 µl of yeast RNA (standard solution - 1 mg/ml). As a control (KS), 25 µL of distilled water was used. Samples were incubated at 37°C for 15 minutes. Then the samples were placed on ice, 50 µl of 0.75% uranyl acetate

solution was added to them and incubated for 10 minutes. The samples were then centrifuged for 2 minutes at 12000 rpm. A sediment formed at the bottom of the Eppendorf; the supernatant was collected in an amount of 200 µl. The supernatant was diluted 20 times with distilled water (200 µl of supernatant + 3800 µl of water) and the optical density was measured at 260 nm on a SmartSpec Plus spectrophotometer (Bio-Rad).

RNAse activity was calculated using the formula:

RNAse act. = (optical density of the test sample - optical density of control) × 1000 × 2000 (dilution factor)

Computational Calculations.

A model of **5** was generated using *Spartan '20*[69]and geometry optimised by molecular mechanics. The structure of binase with bound sulfate was retrieved from the Brookhaven protein database (PDB ID: 1gov)[56]. AutoDock 4.2.6[70] was used to remove water molecules and add hydrogen atoms. Four of the pillar[5]arene's sulfate termini were removed and the molecule manually docked with binase using *Spartan '20* such that the four protein-bound sulfate anions could be attached in their place. The complex was subjected to geometry optimisation using the MMFF.

Detailed information of physical-chemical characterization is presented in Electronic Supporting Information (ESI).

ASSOCIATED CONTENT

Structural characterization, figures with ^{1}H, ^{13}C NMR, FT-IR, MALDI-TOF spectra of all compounds synthesized, the detailed experimental results for the determination of the

association constants between the hosts and the guests are available free of charge via the Internet at http:// pubs.acs.org. (PDF)

AUTHOR INFORMATION

Corresponding Author

Ivan I. Stoikov

E-mail: Ivan.Stoikov@mail.ru

Fax: +7-8432-752253

Tel: +7-8432-337463

Dmitriy N. Shurpik

E-mail: dnshurpik@mail.ru

Fax: +7-8432-752253

Tel: +7-8432-337463

Author Contributions

The manuscript was written through contributions of all authors. All authors have given approval to the final version of the manuscript.

Funding Sources

The work was supported by the Russian Science Foundation (Grant No 17-13-01208).

Notes

The authors declare no competing financial interest

ACKNOWLEDGMENTS

The investigation of structure of the compounds by NMR spectroscopy was carried out within the framework of the grant of the President of the Russian Federation for state support of leading scientific schools of the Russian Federation (NSh-2499.2020.3).

ABBREVIATIONS

FITC, fluorescein isothiocyanate; DLS, dynamic light scattering; UV-*vis*, ultraviolet–visible spectroscopy; DMF, dimethylformamide; DMSO, dimethyl sulfoxide; DDS, drug delivery system; PDI, polydispersity index; BOC group, *tert*-butyloxycarbonyl protecting group; DIPEA, diisopropylethylamine; MALDI, matrix assisted laser desorption/ionization; ESI, electrospray ionization; TEM, transmission electron microscopy; CD, circular dichroism.

REFERENCES

(1) Sun, J., Wei, Q., Zhou, Y., Wang, J., Liu, Q., Xu, H. (2017) A systematic analysis of FDA-approved anticancer drugs. *BMC Syst. Biol*. *11*, 1-17.

(2) Cheng, L., Yang, L., Meng, F., Zhong, Z. (2018) Protein nanotherapeutics as an emerging modality for cancer therapy. *Adv. Healthc. Mater.* 7, 1800685.

(3) Zhu, Q., Chen, X., Xu, X., Zhang, Y., Zhang, C., Mo, R. (2018) Tumor-specific self-degradable nanogels as potential carriers for systemic delivery of anticancer proteins. *Adv. Funct. Mater. 28*, 1707371.

(4) Chalamaiah, M., Yu, W., Wu, J. (2018) Immunomodulatory and anticancer protein hydrolysates (peptides) from food proteins: A review. *Food Chem. 245*, 205-222.

(5) Karpiński, T. M., Adamczak, A. (2018) Anticancer activity of bacterial proteins and peptides. *Pharmaceutics.* 10, 54.

(6) Dyer, K. D., Rosenberg, H. F., (2006) The RNase a superfamily: generation of diversity and innate host defense. *Mol. Divers. 10*, 585-597.

(7) Fang, E. F., Ng, T. B. (2011) Ribonucleases of different origins with a wide spectrum of medicinal applications. Biochim. Biophys. *Acta Rev. Cancer. 1815*, 65-74.

(8) Khodzhaeva, V., Makeeva, A., Ulyanova, V., Zelenikhin, P., Evtugyn, V., Hardt, M., Rozhina, E., Lvov, Y., Fakhrullin, R., Ilinskaya, O. (2017) Binase immobilized on halloysite nanotubes exerts enhanced cytotoxicity toward human colon adenocarcinoma cells. *Frontiers in pharmacol. 8*, 631.

(9) Ulyanova, V., Dudkina, E., Nadyrova, A., Kalashnikov, V., Surchenko, Y., Ilinskaya, O. (2021) The Cytotoxicity of RNase-Derived Peptides. *Biomolecules. 11,* 16.

(10) Cabrera-Fuentes, H. A., Aslam, M., Saffarzadeh, M., Kolpakov, A., Zelenikhin, P., Preissner, K. T., Ilinskaya, O. N. (2013) Internalization of Bacillus intermedius ribonuclease (BINASE) induces human alveolar adenocarcinoma cell death. *Toxicon. 69*, 219-226.

(11) Dudkina, E. V., Ulyanova, V. V., Ilinskaya, O. N. (2020) Supramolecular organization as a factor of ribonuclease cytotoxicity. *Acta Naturae 12*, 24-33.

(12) Braegelman, A. S., Webber, M. J. (2019) Integrating stimuli-responsive properties in host-guest supramolecular drug delivery systems. *Theranostics 9*, 3017–3040.

(13) Li, H., Yang, Y., Xu, F., Liang, T., Wen, H., Tian, W. (2019) Pillararene-based supramolecular polymers. *Chem. Commun. 55,* 271-285.

(14) Cui, Y. H., Deng, R., Li, Z., Du, X. S., Jia, Q., Wang, X. H., Wang, C. Y., Meguellati, K., Yang, Y. W. (2019) Pillar[5]arene pseudo[1]rotaxane-based redox-responsive supramolecular vesicles for controlled drug release. *Mater. Chem. Front. 3,* 1427-1432.

(15) Yang, H.-L., Dang, Z.-J., Zhang, Y.-M., Wei, T.-B., Yao, H., Zhu, W., Fan, Ya.-Q., Jiang, X.-M., Lin, Q. (2019) Novel cyanide supramolecular fluorescent chemosensor constructed from a quinoline hydrazone functionalized-pillar[5]arene. *Spectrochim. Acta A Mol. Biomol. Spectrosc. 220,* 117136.

(16) Song, N., Lou, X. Y., Ma, L., Gao, H., Yang, Y. W. (2019) Supramolecular nanotheranostics based on pillarenes. *Theranostics. 9*, 3075-3093.

(17) Guo, F., Xia, T., Xiao, P., Wang, Q., Deng, Z., Zhang, W., Diao, G. (2021) A supramolecular complex of hydrazide-pillar[5]arene and bisdemethoxycurcumin with potential anti-cancer activity. *Bioorg. Chem. 110*, 104764.

(18) Shurpik, D. N., Sevastyanov, D. A., Zelenikhin, P. V., Subakaeva, E. V., Evtugyn, V. G., Osin, Y. N., Cragg, P. J., Stoikov, I. I. (2018) Hydrazides of glycine-containing decasubstituted pillar[5]arenes: Synthesis and encapsulation of Floxuridine. *Tetrahedron Lett. 59,* 4410-4415.

(19) Shurpik, D. N., Sevastyanov, D. A., Zelenikhin, P. V., Padnya, P. L., Evtugyn, V. G., Osin, Y. N., Stoikov, I. I. (2020) Nanoparticles based on the zwitterionic pillar [5] arene and Ag^{+}: synthesis, self-assembly and cytotoxicity in the human lung cancer cell line A549. B*eilstein J. Nanotechnol. 11*, 421-431.

(20) Shurpik, D. N., Aleksandrova, Yu. I., Zelenikhin, P. V., Subakaeva, E. V., Cragg, P. J., Stoikov, I. I. (2020) Towards new nanoporous biomaterials: self-assembly of sulfopillar[5]arenes with vitamin D3 into supramolecular polymers. *Org. Biomol. Chem. 18*, 4210-4216.

(21) Shurpik, D. N., Mostovaya, O. A., Sevastyanov, D. A., Lenina, O. A., Sapunova, A. S., Voloshina, A. D., Petrov, K. A., Kovyazina, I. V., Cragg, P. J., Stoikov, I. I. (2019) Supramolecular neuromuscular blocker inhibition by a pillar[5]arene through aqueous inclusion of rocuronium bromide. *Org. Biomol. Chem. 17*, 9951-9959.

(22) Tuo, W., Sun, Y., Lu, S., Li, X., Sun, Y., Stang, P. J. (2020) Pillar[5]arene-containing metallacycles and host–guest interaction caused aggregation-induced emission enhancement platforms. *J. Am. Chem. Soc. 142*, 16930-16934.

(23) Guo, C., Sedgwick, A. C., Hirao, T., Sessler, J. L. (2021) Supramolecular fluorescent sensors: An historical overview and update. *Coord. Chem. Rev. 427*. 213560.

(24) Yang, K., Zhang, Z., Du, J., Li, W., Pei, Z. (2020) Host–guest interaction based supramolecular photodynamic therapy systems: a promising candidate in the battle against cancer. *Chem. Commun. 56*, 5865-5876.

(25) Sun, J., Dai, Y., Hou, Y., Wu, Q., Ma, L., Zhao, J., Wang, B. (2021) Weakened triplet–triplet annihilation of diiodo-BODIPY moieties without influence on their intrinsic triplet lifetimes in diiodo-BODIPY-functionalized pillar[5]arenes. *J. Phys. Chem. A. 125*, 2344-2355.

(26) Strutt, N. L., Zhang, H., Schneebeli, S. T., Stoddart, J. F. (2014) Functionalizing pillar[n]arenes. *Acc. Chem. Res. 47*, 2631-2642.

(27) Strutt, N. L., Forgan, R. S., Spruell, J. M., Botros, Y. Y., Stoddart, J. F. (2011) Monofunctionalized pillar[5]arene as a host for alkanediamines. *J. Am. Chem. Soc. 133*, 5668-5671.

(28) Han, C., Zhang, Z., Yu, G., Huang, F. (2012) Syntheses of a pillar[4]arene[1]quinone and a difunctionalized pillar [5] arene by partial oxidation. *Chem. Commun. 48*, 9876-9878.

(29) Ogoshi, T., Demachi, K., Kitajima, K., Yamagishi, T. A. (2011) Monofunctionalized pillar[5]arenes: synthesis and supramolecular structure. *Chem. Commun. 47*, 7164-7166.

(30) Steffen, A., Thiele, C., Tietze, S., Strassnig, C., Kämper, A., Lengauer, T., Wenz, G., Apostolakis, J. (2007) Improved Cyclodextrin Based Receptors for Camptothecin by Inverse Virtual Screening. *Chem.-Eur. J. 13*, 6801-6809.

(31) Knoblauch, S., Falana, O. M., Nam, J., Roundhill, D. M., Hennig, H., Zeckert, K. (2000) Calix[4]arenes with narrow rim 2-mercaptoethoxy substituents as potential precursor molecules for metallacages and sensors. *Inorganica Chim. Acta. 300*, 328-332.

(32) Šnejdárková, M., Poturnayová, A., Rybár, P., Lhoták, P., Himl, M., Flídrová, K., Hianik, T. High sensitive calixarene-based sensor for detection of dopamine by electrochemical and acoustic methods. Bioelectrochemistry. 80 (2010) 55-61.

(33) Zhang, F., Ma, J., Sun, Y., Boussouar, I., Tian, D., Li, H., Jiang, L. (2016) Fabrication of a mercaptoacetic acid pillar[5]arene assembled nanochannel: a biomimetic gate for mercury poisoning. *Chem. Sci. 7*, 3227-3233.

(34) Lukášek, J., Böhm, S., Dvořáková, H., Eigner, V., Lhoták, P. (2014) Regioselective halogenation of thiacalix[4]arenes in the *cone* and *1,3-alternate* conformations. *Org. Lett. 16*, 5100-5103.

(35) Kundrat, O., Dvorakova, H., Eigner, V., Lhotak, P. (2010) Uncommon regioselectivity in the thiacalix[4]arene series: gross formylation of the *cone* conformer. *J. Org. Chem. 75*, 407-411.

(36) Kumar, R., Lee, Y. O., Bhalla, V., Kumar, M., Kim, J. S. (2014) Recent developments of thiacalixarene based molecular motifs. *Chem. Soc. Rev. 43*, 4824-4870.

(37) Yao, Y., Xue, M., Chi, X., Ma, Y., He, J., Abliz, Z., Huang, F. (2012) A new water-soluble pillar[5]arene: synthesis and application in the preparation of gold nanoparticles. *Chem. Commun. 48*, 6505-6507.

(38) Traboulsi, H., Larkin, H., Bonin, M. A., Volkov, L., Lavoie, C. L., Marsault, E. (2015) Macrocyclic cell penetrating peptides: a study of structure-penetration properties. *Bioconjugate Chem. 26*, 405-411.

(39) Reibarkh, M. Y., Nolde, D. E., Vasilieva, L. I., Bocharov, E. V., Shulga, A. A., Kirpichnikov, M. P., Arseniev, A. S. (1998) Three-dimensional structure of binase in solution. *FEBS letters 431*, 250-254.

(40) https://www.rcsb.org/3d-view/1BUJ. Accessed on xx/yy/zz

(41) Feng, W., Jin, M., Yang, K., Pei, Y., Pei, Z. (2018) Supramolecular delivery systems based on pillararenes. *Chem. Commun. 54*, 13626-13640.

(42) Stubbe, J., Kozarich, J. W. (1987) Mechanisms of bleomycin-induced DNA degradation. *Chem. Rev. 87*, 1107-1136.

(43) Griswold, K. E., Bement, J. L., Teneback, C. C., Scanlon, T. C., Wargo, M. J., Leclair, L. W. (2014) Bioengineered lysozyme in combination therapies for Pseudomonas aeruginosa lung infections. *Bioengineered 5*, 143-147.

(44) Damaghi, M., Wojtkowiak, J. W., Gillies, R. J. (2013) pH sensing and regulation in cancer. *Front. Physiol. 4*, 370.

(45) Webb, B. A., Chimenti, M., Jacobson, M. P., Barber, D. L. (2011) Dysregulated pH: a perfect storm for cancer progression. *Nat. Rev. Cancer. 11*, 671-677.

(46) Erlanson, C., Borgström, B. (1970) Tributyrine as a substrate for determination of lipase activity of pancreatic juice and small intestinal content. *Scand. J. Gastroenterol. 5*, 293-295.

(47) Hibbert, D. B., Thordarson, P. (2016) The death of the Job plot, transparency, open science and online tools, uncertainty estimation methods and other developments in supramolecular chemistry data analysis. *Chem. Commun. 52*, 12792-12805.

(48) Bindfit; http://supramolecular.org. Accessed on xx/yy/zz

(49) Li, C., Ma, J., Zhao, L., Zhang, Y., Yu, Y., Shu, X., Li, J., Jia, X. (2013) Molecular selective binding of basic amino acids by a water-soluble pillar[5]arene. *Chem. Commun. 49*, 1924-1926.

(50) Chen, Y., Fu, L., Sun, B., Qian, C., Wang, R., Jiang, J., Wang, L. (2020) Competitive selection of conformation chirality of water-soluble pillar[5]arene induced by amino acid derivatives. *Org. Lett. 22*, 2266-2270.

(51) Shu, X., Xu, K., Hou, D., Li, C. (2018) Molecular recognition of water-soluble pillar[n]arenes towards biomolecules and drugs. *Isr. J. Chem. 58*, 1230-1240.

(52) Ermakova, E. (2007) Brownian dynamics simulation of the competitive reactions: binase dimerization and the association of binase and barstar. *Biophys. Chem. 130*, 26-31.

(53) Okorokov, A. L., Panov, K. I., Offen, W. A., Mukhortov, V. G., Antson, A. A., Ya. M., Karpeisky, Wilkinson, A. J., Dodson, G. G. (1997) RNA cleavage without hydrolysis. Splitting the catalytic activities of binase with Asn101 and Thr101 mutations. *Protein Eng. 10*, 273-278.

(54) Pang, Y., Buck, M., Zuiderweg, E. R. (2002) Backbone dynamics of the ribonuclease binase active site area using multinuclear (^{15}N and ^{13}CO) NMR relaxation and computational molecular dynamics. *Biochemistry 41*, 2655-2666.

(55) Brooks III, C. L., Karplus, M. (1989) Solvent effects on protein motion and protein effects on solvent motion: dynamics of the active site region of lysozyme. *J. Mol. Biol. 208*, 159-181.

(56) Polyakov, K. M., Lebedev, A. A., Okorokov, A. L., Panov, K. I., Schulga, A. A., Pavlovsky, A. G., Karpeisky, M. Y. A., Dodson, G. G. (2002) The structure of substrate-free microbial ribonuclease binase and of its complexes with 3'GMP and sulfate ions. *Acta Crystallogr. D Biol. Crystallogr. 58*, 744-750.

(57) Zhuang, Y. D., Chiang, P. Y., Wang, C. W., Tan, K. T. (2013) Environment sensitive fluorescent turn on probes targeting hydrophobic ligand binding domains for selective protein detection. *Angew. Chem. Int. Ed. 125*, 8282-8286.

(58) Salem, J. K., El-Nahhal, I. M., Salama, S. F. (2019) Determination of the critical micelle concentration by absorbance and fluorescence techniques using fluorescein probe. *Chem. Phys. Lett. 730*, 445-450.

(59) Lakowicz, J. R. (Ed.) (2013) Principles of fluorescence spectroscopy, Springer science & business media.

(60) Patil, V. S., Padalkar, V. S., Tathe, A. B., Sekar, N. (2013) ESIPT-inspired benzothiazole fluorescein: Photophysics of microenvironment pH and viscosity. *Dyes Pigm. 98*, 507-517.

(61) Afzal, S., Lone, M. S., Bhat, P. A., Dar, A. A. (2018) Multi-step fluorescence resonance energy transfer between the fluorophores via cosolubilization in cationic, anionic and non-ionic micelles. *J. Photoch. Photobio. A. 365*, 220-231.

(62) Sjöback, R., Nygren, J., Kubista, M. (1995) Absorption and fluorescence properties of fluorescein. *Spectrochim. Acta A Mol. Biomol. Spectrosc. 51*, L7-L21.

(63) Lin, C. H., Wen, H. C., Chiang, C. C., Huang, J. S., Chen, Y., Wang, S. K. (2019) Polyproline tri-helix macrocycles as nanosized scaffolds to control ligand patterns for Selective protein oligomer interactions. *Small*, *15* 1900561.

(64) M. Bojtár, J. Kozma, Z. Szakács, D. Hessz, M. Kubinyi, I. Bitter (2017) Pillararene-based fluorescent indicator displacement assay for the selective recognition of ATP. *Sens. Actuators B Chem*, *248*, 305-310.

(65) K. Yang, Y. Pei, J. Wen, Z. Pei (2016) Recent advances in pillar[n]arenes: synthesis and applications based on host–guest interactions. *Chem. Commun.*, *52*, 9316-9326.

(66) Porta, C., Paglino, C., Mutti, L. (2008) Ranpirnase and its potential for the treatment of unresectable malignant mesothelioma. *Biol.: Targets Ther. 2*, 601.

(67) Mosmann, T. (1983). Rapid colorimetric assay for cellular growth and survival: application to proliferation and cytotoxicity assays. *J. Immunol. Methods, 65(1-2)*, 55-63.

(68) Anfinsen, Jr, C. B. (1957) Structural basis of ribonuclease activity. *Fed. Proc. 16*, 783-791.

(69) *Spartan '20* (v 1.1.1), Wavefunction Inc., 18401 Von Karman Ave., Suite 435, Irvine, CA 92612, USA

(70) Morris, G. M., Huey, R., Lindstrom, W., Sanner, M. F., Belew, R. K., Goodsell, D. S., Olson, A. J. (2009) Autodock4 and AutoDockTools4: automated docking with selective receptor flexibility. *J. Comput. Chem. 16*, 2785-91.

BRIEF ABSTRACT

Pillar[5]arenes containing sulfonate fragments have been shown to form supramolecular complexes with therapeutic proteins to facilitate targeted transport with an increased duration of action and enhanced bioavailability.

For Table of Contents only